San Jose State University

SJSU ScholarWorks

8-1-2021

Extreme fire weather associated with nocturnal drying in elevated coastal Terrain of California

Richard B. Bagley
San Jose State University

Craig B. Clements
San Jose State University, craig.clements@sjsu.edu

Follow this and additional works at: https://scholarworks.sjsu.edu/faculty_rsca

Extreme Fire Weather Associated with Nocturnal Drying in Elevated Coastal Terrain of California

RICHARD B. BAGLEY[a,b] AND CRAIG B. CLEMENTS[a]

[a] *Fire Weather Research Laboratory, Department of Meteorology and Climate Science, San José State University, San Jose, California*
[b] *Pacific Gas and Electric Company, San Francisco, California*

ABSTRACT: The second largest fire shelter deployment in U.S. history occurred in August 2003 during the Devil Fire, which was burning in a remote and rugged region of the San Francisco Bay Area, when relative humidity abruptly dropped in the middle of the night, causing rapid fire growth. Nocturnal drying events in the higher elevations along California's central coast are a unique phenomenon that poses a great risk to wildland firefighters. Single-digit relative humidity with dewpoints below $-25°C$ is not uncommon during summer nights in this region. To provide the fire management community with knowledge of these hazardous conditions, an event criterion was established to develop a climatology of nocturnal drying and to investigate the synoptic patterns associated with these events. A lower-tropospheric source region of dry air was found over the northeastern Pacific Ocean corresponding to an area of maximum low-level divergence and associated subsidence. This dry air forms above a marine inversion and advects inland overnight with the marine layer and immerses higher-elevation terrain with warm and dry air. An average of 15–20 nocturnal drying events per year occur in elevations greater than 700 m in the San Francisco Bay Area, and their characteristics are highly variable, making them a challenge to forecast.

KEYWORDS: Synoptic climatology; Wildfires; Automatic weather stations; Coastal meteorology; Forest fires

1. Introduction

Extreme fire weather is commonly associated with adverse firefighting conditions that can at times result in fire shelter deployments and even fatalities. On 29 August 2003 the largest fire shelter deployment in California and second largest in the United States occurred just after midnight during the Devil Fire, which was burning in the mountains east of the San Francisco Bay Area (SFBA). Sudden atmospheric drying and onset of single-digit relative humidity above the marine layer led to a dramatic increase in fire activity that trapped 51 firefighters and two bulldozer operators, forcing them to take emergency cover in a self-contained fire-resistant shelter. The fire shelter is a personal safety device carried by all wildland firefighters and is used for cover only as a last resort in case of entrapment.

The amount of moisture in the atmosphere has long been recognized for its contribution to fire behavior (Munns 1921; Potter 2012; Werth et al. 2011). Low atmospheric moisture impacts fuels by reducing the fuel moisture content of a range of fuel classes based on their diameter and this relationship has become the key factor in fire danger rating systems around the world (Cohen and Deeming 1985). Along with fire danger rating, various fire weather indices have been developed over the years that have focused mainly on surface wind speed and

humidity (e.g., Fosberg 1978; Srock et al. 2018), while Haines (1989) suggested using midlevel moisture and instability as a means to deduce potential for large fire growth.

Large-scale weather patterns and upper-level features have also proven critical to the fire behavior (Brotak and Reifsnyder 1977; Werth et al. 2011). Common synoptic patterns associated with critical fire weather in California and have been well known in the wildfire community include the subtropical high aloft (500 hPa), a meridional ridge with southwesterly flow, a postfrontal Pacific high, and the Great Basin high (Schroeder et al. 1964; Werth et al. 2011). While subtropical high pressure was responsible for the most number of high fire danger days in California because of intense warming, effectiveness in blocking moisture, and frequency of occurrence, the Great Basin high has long been recognized as the most critical pattern because of its role in producing the Santa Ana and Diablo winds associated with strong offshore flow and low relative humidity (RH) (Huang et al. 2009; Hughes and Hall 2010; Raphael 2003).

A similar extreme reduction in surface humidity (<10%) was observed during two devastating southern Australia fires in 2003 and 2005 (Mills 2008a, b). Mills (2008a) found a two-part process responsible for transporting dry upper-tropospheric air to the surface. The first phase consisted of jet stream entrance and exit circulations that brought upper-level dry air into the midtroposphere. The second phase included a deep well-mixed boundary layer through which dry convection entrained low humidity air to near-surface levels. While the first phase lasted for hours, the second phase of boundary layer mixing took place in less than an hour. A preliminary climatology of southern Australia drying events spanning six fire seasons was also conducted (Mills 2008b). A drying event was

categorized as having dewpoints less than −5°C or dewpoints less than −2.5° and RH less than 10%. To further refine event abruptness, an event score was based on dewpoint variance, range, and deviation. Most events observed during this study occurred between midmorning and early evening local time and were associated with spatial and temporal coherence that was identified with nearby stations simultaneously reporting drying event criteria, indicative of large-scale forcing.

During the summer months of June, July, and August, coastal California is associated with stratus and fog that advects into interior valleys regulating the climate of the region. The formation of stratus involves an inversion that gradually decreases in height from west to east across the northeastern Pacific Ocean with a base at 2 km over the Hawaiian Islands and reaches its lowest point of ~400 m along the California coast (Neiburger 1960). A semipermanent anticyclone centered near 38°N and 150°W was responsible for this large-scale feature through subsidence and low-level divergence along its eastern boundary. The prevailing north-northwesterly flow along the U.S. West Coast was the primary mechanism for fog and stratus production as well as the corresponding capping inversion. The main processes involved are discussed in Pilié et al. (1979). Initial stratus-free environments occur when offshore winds pushed dry air out to sea and destroy the moist marine boundary layer. As winds return to their mean direction of 330°, continued subsidence lowers the inversion to near-surface levels and effectively traps moist air near the ocean–atmosphere interface. However, the large-scale subsidence also results in a much warmer and drier environment immediately above the shallow marine inversion.

While coastal California is subject to stratus and fog during summer, there exists a unique phenomenon in which higher elevations above the marine layer can become immersed in extremely dry air during the overnight hours. Between 925 and 850 hPa, the subsidence inversion above the west coast marine layer can be composed of air with mixing ratios as low as $0.5 \, \mathrm{g \, kg^{-1}}$ and dewpoint temperatures below −25°C. Combined with increased temperatures and lack of moisture, the inversion above a marine layer often heralds extreme fire danger at upper elevations. Single-digit relative humidity is not uncommon in the highest SFBA peaks and ridges during summer nights as was observed during the Devil Fire.

The Devil Fire was part of the Santa Clara Complex actively burning in a remote area of the Diablo Range 11 km south of Livermore, California. The fire originally started from an intense convective outbreak roughly 48 h prior that resulted in 81 lightning strikes over the Diablo Range between 2200 and 0000 Pacific daylight time (PDT) 26 August 2003 as observed by National Lightning Detection Network (Walbrun and Blier 2004). By the next day, a group of 23 fires collectively known as the Santa Clara Complex would go on to burn 12 550 ha. Nearly 48 h after the first lightning strike, the largest emergency fire shelter deployment in California history and second largest in U.S. history took place when a fire overran fire crews battling the Devil Fire in a remote and rugged portion of the northern Diablo Range.

According to a California Department of Forestry and Fire Protection Review (California Department of Forestry and Fire Protection 2003), at approximately 0115 PDT 29 August 2003, two California Department of Forestry (CDF) overhead personnel, two dozer operators, and 51 CDF Inmate Conservation Camp Fire Crew firefighters become entrapped while performing a holding operation along a ridge at 1100 m MSL near Eylar Mountain. During the entrapment, 53 fire shelters were successfully deployed while the two dozer operators took refuge in their enclosed cabs. The only injuries were second degree burns less than 2 cm in diameter experienced by two CDF employees and one inmate firefighter.

The crew was reassigned to the fire earlier in the evening and made their way up a ridge to support a planned firing operation to assist in containment by eliminating fuels ahead of the fire front. The main fire was burning in a canyon below, and the fire behavior that evening was described as low intensity to moderate while making short uphill runs. The firing operation began at approximately 2235 PDT and was terminated shortly after midnight when crews could not get fire to ignite. At approximately the same time, the main fire became active as RH lowered and winds turned from a westerly to a north-northwesterly direction, aligning with the direction of the canyon. Flame lengths of 9–15 m were observed until the fire reached brush fuel in slopes of 70%–80%, and flame lengths then increased to 30 m. Rapid upslope runs, some in excess of 300 m over a 2–3-min period, and spot fires over 400 m ahead of the fire were also observed. As the fire spread upslope toward the crew and it was realized they could not make it to a designated safety zone, a firing operation was carried out surrounding the perimeter of the shelter deployment site in an area of lighter fuels. The deployment lasted for 10–15 min.

The counterintuitiveness of this event is twofold. In general, fire management agencies expect fire behavior and activity to lessen at night as RH recovers with decreasing nighttime temperatures. Second, these events are usually above a higher moisture environment with stratus clouds or fog, which has the opposite effect on fire activity, and only a shallow inversion consisting of steep temperature and dewpoint lapse rates separates the two. During nocturnal drying events (NDEs), RH peaks during the afternoon and decreases to the lowest values overnight across elevated terrain.

The motivation of this research is to better understand nocturnal drying as it pertains to fire behavior and fire danger in the complex terrain of California. Although local land managers and fire agencies have long recognized the potential for more active fire growth in the elevated coastal topography of the SFBA and central California during nighttime, knowledge remains mostly anecdotal and there has been very little investigation into the meteorological factors behind such events, let alone the frequency or extent of occurrence. The ambiguity surrounding nocturnal drying also makes forecasting a challenge when necessary. In this paper, we look into the meteorological factors resulting in the rapid growth of the Devil Fire and construct a climatology of higher-elevation Bay Area Remote Automated Weather Stations (RAWS) to help establish a basic set of criteria and determine how often NDEs occur in the SFBA as well as the rest of California. The average number of events per summer in California between 2000 and 2014 was identified using data from RAWS at various
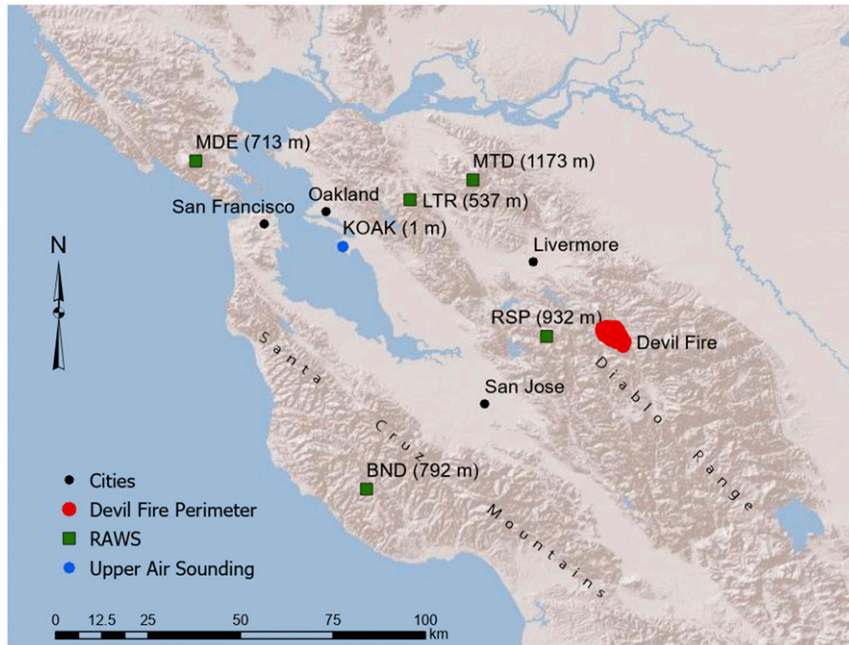
FIG. 1. Shaded-relief map of the SFBA, Devil Fire location, four primary RAWS, and launch site of KOAK upper-air soundings.

elevations generally above 500 m. A synoptic composite was then developed to determine the source region of dry air and how large-scale momentum, temperature, and moisture variables evolve in the days before and after significant, widespread NDEs in the SFBA. In section 2, we present the methods and study design, followed by the results in section 3, and summary and conclusions in section 4.

2. Methods and study design

a. Observed meteorological conditions during the Devil Fire

An initial investigation into the meteorological conditions surrounding the Devil Fire was performed first using data from the nearby Rose Peak RAWS and upper-air soundings from Oakland International Airport (KOAK) (Fig. 1). A summary report of the fire shelter deployment by California Department of Forestry and Fire Protection provided useful information about the fire behavior during the entrapment. To help to locate a source region of the extremely dry air, a 27-member ensemble backward trajectory was calculated using the HYSPLIT atmospheric transport and dispersion model, version 5.0.0. Each 24-h backward trajectory ensemble is calculated by offsetting the original starting location by one grid point in the horizontal and 0.01 sigma units in the vertical and was initialized using North American Regional Reanalysis (NARR) 32-km data. Start time was set at 0200 PDT 28 August 2003 for the location of the fire shelter deployment at an elevation of 1100 m.

b. Event criteria and climatology

To determine what qualifies as a nocturnal drying event, a basic set of threshold criteria was established that was partially based on surface meteorological conditions corresponding to the time of extreme fire behavior and subsequent overrunning of the Devil Fire during the night of 29 August 2003. According to the nearby Rose Peak RAWS, RH values between 20% and 30% were reported that evening, and then shortly after 0100 PDT, RH suddenly dropped to single digits during the time of deployment. Dewpoint temperatures also plunged to a range from $-10°$ to $-15°C$ or lower from the onset of explosive fire growth until sunrise.

However, since fire history associated with NDEs is so limited, further refinement of moisture variables used for event criteria was needed to identify moisture thresholds that are representative of more extreme scenarios in this region. Persistently warm and dry conditions are common above the marine layer and in the higher elevations of the SFBA during the summer months, making it a naturally lower RH environment, with values between 15% and 30% not uncommon. Therefore, a dewpoint temperature threshold was desired to better gauge atmospheric aridity because that is the main factor responsible for the rapid drying of finer fuels and corresponding explosive fire growth.

Since nocturnal drying is usually observed in terrain above 500 m, a preliminary analysis using data from high-elevation SFBA RAWS was performed to build a climatology of moisture variables between 1 May and 31 October from 2000 to 2014. Although there are only four RAWS in the greater SFBA above 700 m with sufficient history, they are all located near or atop a peak or ridge and are evenly distributed around the various SFBA mountain ranges to represent an areal coverage of over 3000 km^2 (Fig. 1). Located at 713 m along a ridge near the peak of Mount Tamalpais, MDP is the northwesternmost site of the four. Farther south, along the coast and above the town of Ben Lomond, BND is situated atop a far western spine

TABLE 1. Listing by region of stations used in climatology of NDEs from 2000 to 2014. Here ID indicates the station identifier.

Station (region)	Elev (m MSL)	Lat (°)	Lon (°)	ID	Event count May–Oct
Coastal Northern California (NC)					
Cooskie Mountain	898	40.26	−124.27	PTE	4
Hawkeye	617	38.74	−122.84	HWK	1
Mendocino Pass	1640	39.81	−122.95	MAS	2
Slater Butte	1409	41.86	−123.35	ATR	2
Yolla Bolla	1366	40.34	−123.07	YOB	1
San Francisco Bay Area (SFBA)					
Mount Diablo	1173	37.88	−121.91	MTD	37
Rose Peak	933	37.50	−121.74	RSP	22
Ben Lomond	792	37.13	−122.17	BND	14
Middle Peak	713	37.93	−122.59	MDE	15
Atlas Peak	590	38.47	−122.26	ATL	2
Big Rock	457	38.04	−122.57	NBR	1
Las Trampas	537	38.83	−122.07	LTR	2
Diablo Grande	567	37.33	−121.30	DBL	2
Los Gatos	561	37.20	−121.95	LSG	4
Cordoza Ridge	711	37.17	−121.53	TT119	2
Coastal Central California (CC)					
Figueroa	970	34.73	−120.01	FGM	5
Highlands Peak	759	36.07	−121.56	HPE	13
Southern California (SC)					
Mount Wilson	1740	34.23	−118.07	MWS	27
Camp 9	1219	34.35	−118.42	CNI	14
Malibu Hills	480	34.06	−118.65	MBU	3
Alpine	857	32.84	−116.67	ANE	3
Otay Mountain	1001	32.60	−116.84	OTY	13
Sierra Nevada (SN)					
Carpenter Ridge	1468	40.07	−121.584	CDE	2
Pike County Lookout	1128	39.47	−121.202	PKC	1
Duncan	2164	39.14	−120.51	DUC	1
Mount Tom	2738	37.38	−119.18	MMT	4
Mountain Rest	1253	37.05	−119.37	MTQ	0

of the Santa Cruz Mountains at an elevation of 792 m. Representing the interior mountains of the SFBA are Mount Diablo (MTD) and Rose Peak (RSP). Perched atop the summit of conically shaped Mount Diablo (1173 m MSL), MTD is the highest and most exposed location of the four RAWS. Rose Peak RAWS is located on an upper, west-facing slope at 933 m in the northern portion of the expansive Diablo Range and is the most sheltered of the four sites.

Quality control of RAWS data included removal of data outside a well-defined range of reasonable values for each variable. Further data quality assurance was performed by visually inspecting annual time series plots of temperature, dewpoint, and RH for any outlying values.

This analysis revealed 5–10th-percentile summertime dewpoints averaging around −10°C across stations and 5–10th-percentile summer relative humidity values near 10%. Given that these values were similar to the conditions during the explosive growth of the Devil Fire, a basic set of qualifiers using single-digit relative humidity in conjunction with dewpoint temperatures at or below −10.0°C was used to identify nocturnal drying. However, since extreme drying can start and end abruptly, often more than once in 24 h, and can persist on the scale of hours

or days, a minimum time duration of 3 h was required to be considered as an event. Also, a limit of one event per 24 h was set to account for the possibility of multiple events on the same date.

Such meteorological conditions can be considered critical fire weather conditions associated with extreme fire behavior. Similar methods by Mills (2008b) were used involving RH < 10% in combination with dewpoint criteria when evaluating event scores for drying episodes in Australia. Therefore, an NDE is hereby identified as a period of at least 3 h between 2000 and 0800 LT during which RH values below 9.5% accompany dewpoint temperatures less than or equal to −10.0°C.

The above definition was then used to identify how common NDEs are at various upper elevations and locations not only in the SFBA but across the rest of California during the typical wildfire months of 1 May–31 October. An average event count was calculated with data from 27 RAWS using MesoWest (Horel et al. 2002). The majority of stations are scattered across California, with the greatest concentration in the SFBA and Southern California mountains. Five of the stations are in the Sierra Nevada. To sample as much of the free atmosphere as possible above or within proximity to the marine inversion, stations were selected on the basis of their location atop

mountain peaks, ridges, or upper slopes at elevations greater than 450 m (Table 1). For clarity and to distinguish between different climatological exposures to the marine layer, sites are grouped into four regions: Northern California (NC), SFBA, Central California (CC), Southern California (SC), and Sierra Nevada (SN). A total of 12 of the 27 RAWS used in this study have been operable for at least 15 years, and only 5 stations have less than 10 years of data. The same data quality control measures used with the four original SFBA RAWS were applied to the other 23 sites used for event identification.

After identifying the spatial and temporal extent of nocturnal drying in California, a more extensive investigation into the surface meteorological variables surrounding NDEs was then conducted involving five sites from the SFBA. In addition to MDE, MTD, BND, and RSP, another SFBA RAWS was selected to compare conditions in the higher terrain of the SFBA where the population is rural to a more densely populated area. The Las Trampas RAWS (LTR) afforded a good approximation of this wild–urban interface. Located atop a ridge in the eastern edge of the East Bay Hills, LTR (537 m MSL) is representative of middle elevations and is roughly in the geographic center of the SFBA (Fig. 1).

Data analysis of the selected SFBA stations started with how frequent NDEs are on daily and seasonal scales. Histograms were constructed to show the relative frequency of occurrence of NDEs per month on an annual basis and events by hour on a daily basis between 1 May and 31 October. Mean values of pertinent surface weather variables including temperature, winds, dewpoint and RH between 1 May and 31 October were then calculated and compared to mean values of the same variables during previously identified NDEs. Mean values of 10-h fuel moisture were also determined using RAWS 10-h fuel sensors from all five sites. Finally, simultaneous dewpoint depressions between MTD and LTR during NDEs were calculated to see how widely dewpoints can vary over a small horizontal and vertical distance.

c. Composite analysis

There have been instances in which significant overnight drying affects an entire region of the SFBA simultaneously, as well as reaching abnormally low levels. To further understand the circumstances under which more substantial and widespread NDEs occur, a catalog of dates spanning an 11-yr period from 2004 to 2014 was created and then large-scale momentum, temperature, and moisture characteristics of the atmosphere were investigated before, during, and after the most critical periods of nocturnal drying using data from the North American Mesoscale (NAM) Model 218, with 12-km resolution.

The SFBA has an ideal experimental design with a diverse network of RAWS at all elevations, as well as upper-air soundings launched twice daily from Oakland International Airport (KOAK) at 0000 and 1200 UTC (1700 and 0500 PDT) (Fig. 1). Oakland Airport is situated near the geographic center of the SFBA. For this purpose, significant nocturnal drying events were recognized when at least three of the four high elevation SFBA RAWS (MDE, MTD, BND, or RSP) reached NDE criteria on the same date. Furthermore, if two stations
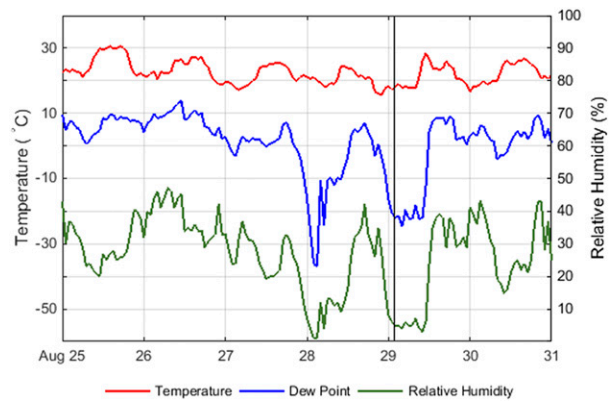
FIG. 2. Time series of temperature and moisture variables from Rose Peak RAWS (RSP) during the days surrounding the Devil Fire shelter deployment at 0115 PDT 29 Aug 2003 as represented by the vertical line.

observed conditions of less than $-20°C$ and 5% for at least 1 h, then that also qualified as a significant NDE. In addition, dewpoint temperatures from the 1200 UTC KOAK sounding were used to verify that 900-hPa dewpoints were less than or equal to $-10°C$, which is near the 5th–10th percentile for the May–October time frame. In all, 87 significant NDEs were identified.

A time of $T = 0$ was established when overnight RH and dewpoint temperatures were at their lowest values during the chosen NDE. Each $T = 0$ then had to be converted to the nearest 6-h interval because of the temporal constraints of the NAM analysis used for compositing, or spatial and temporal averaging of specific meteorological variables. From $T = 0$, 12-h intervals from 36 h before and 12 h after each event were used to show synoptic evolution and are hereby identified as $T - 36$, $T - 12$, and $T + 12$, as done in (Brewer et al. 2012). For cases in which significant nocturnal drying persisted for multiple nights, the first night is considered to be $T = 0$, and $T + 12$ was calculated from the final consecutive night. Using the NAM Model data, composites of these times were created for mean sea level pressure (MSLP); 925-, 850-, 700-, and 500-hPa pressure levels; and corresponding meteorological variables.

d. Upper-air sounding

The early morning KOAK soundings from 0500 PDT often exhibit the NDE signature of large dewpoint depressions above a shallow marine layer. Based on previously identified significant NDEs, corresponding 1200 UTC Oakland soundings were used to create a mean vertical profile of temperature, moisture, and wind variables. Data acquired from University of Wyoming were organized into vertically averaged 10-hPa pressure levels with a surface of 1020 hPa and a top of 100 hPa. Stability and low-level flow diagnostics were then performed at heights above and below the inversion. The height of the inversion is important because it acts to separate the cooler and more humid air mass below the inversion from the warm and dry air mass above it.
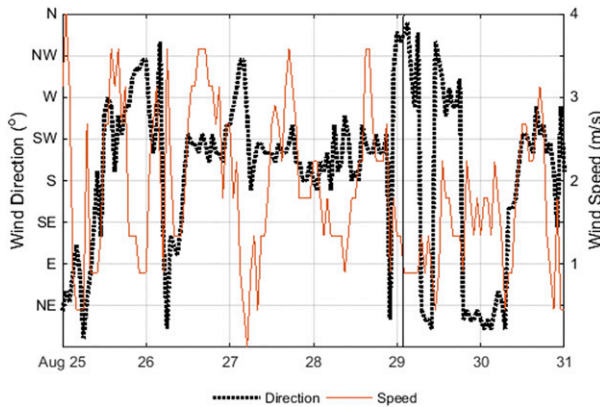
FIG. 3. As in Fig. 2, but for wind speed and direction.

3. Results

a. Observed meteorological conditions during the Devil Fire

A weather summary from the California Department of Forestry and Fire Protection (California Department of Forestry and Fire Protection 2003) described a weak, small-scale trough of low pressure moving across Northern California, increasing the inland extent of the marine layer with a depth of approximately 760 m. Relative humidity values above the marine layer that evening were measured in the 25%–30% range at an elevation of 914 m MSL and dropped between 14% and 20% after midnight. At 0100 PDT, just before the fire shelter deployment, RH values of 6% were documented near the deployment site. Wind speeds were estimated to be 4 m s^{-1}. The nearby Rose Peak RAWS station, also reported an abrupt drop in RH accompanying a shift in winds from a

westerly to northerly direction (Figs. 2 and 3) around midnight on 29 August. After midnight, RH decreased to 5%–10% and did not recover until after sunrise.

There are several features of note that stand out in Fig. 2. First, much lower RH values were recorded during the night prior to the Devil Fire overrunning, with an equally abrupt drop during the same time. Whether this had any effect on fire activity in the area at the time is unknown. Second, decreases in RH correspond closer to dewpoint temperatures than air temperatures, signifying that moisture deficiencies are more important than temperatures in reducing RH. Finally, the diurnal pattern of temperature and dewpoint are generally in phase with each other, which is the opposite of typical diurnal cycles and unique to RAWS in the upper elevations of the SFBA. Dewpoint temperature trends coincide with air temperature trends, reaching maximum values during the daytime and minimum values overnight; to varying degrees.

A general diurnal pattern can also be discerned from wind speed and direction in the days surrounding the Devil Fire incident (Fig. 3). In the days leading up to 29 August, wind speeds peak at RSP around 3.5 m s^{-1} in the late afternoon and reach a minimum overnight through the following morning. Wind direction is southwesterly in the afternoon when wind speeds are at their greatest. Just before 0000 PDT, a transition from westerly to northerly wind coincides with abruptly declining dewpoint temperatures and RH values. Wind speeds decrease from 2.5 m s^{-1} to less than 1 m s^{-1} during the onset of dry air.

The event persisted through 1035 PDT, but within 2 h a rapid humidity recovery back to the 30%–40% range was observed, even though winds remained out of the north until later in the afternoon. Immediately before the transition, there is a slight uptick in wind speed, decrease in dewpoint depression, and increasing RH values; attributes of a weak marine layer or
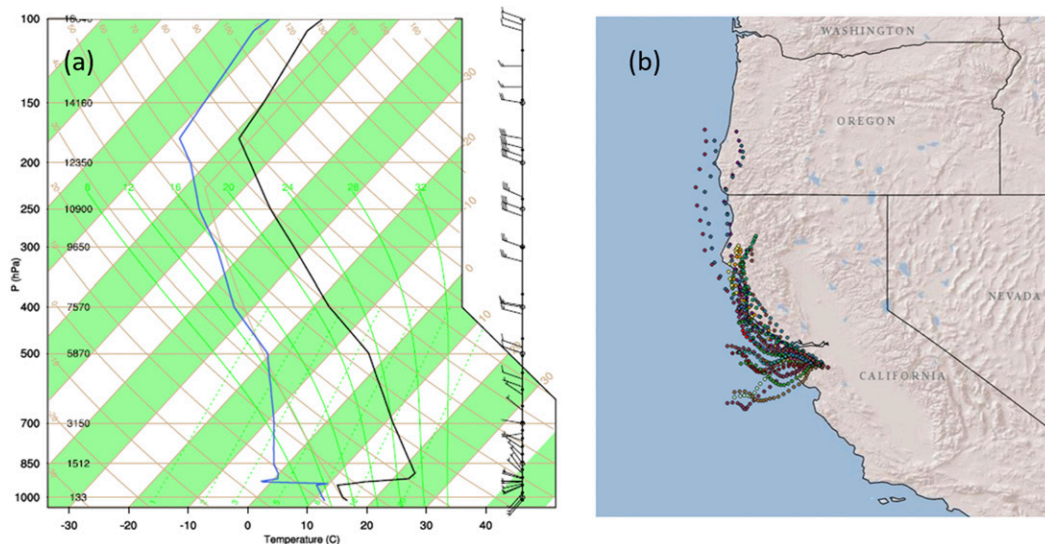
FIG. 4. (a) KOAK upper-air sounding from 0500 PDT 29 Aug 2003 of temperature (black), dewpoint (blue), and wind barbs (m s^{-1}), and (b) 24-h 27-member HYSPLIT backward trajectories from the time of the Devil Fire shelter deployment site.

inversion top. That same signal can be seen a few hours earlier and, to a greater extent, in the evening prior. The maximum temperature from RSP on 28 August was 24.4°C. During the NDE, temperatures varied from 18.9° to 17.2°C before increasing after sunrise. The measurements from RSP match well to the 0500 PDT upper-air sounding from KOAK (Fig. 4a) from 29 August. Here, a sharp inversion is present near 925 hPa (785 m) that separates dewpoint depressions less than 5°C in the marine layer from dewpoint depressions greater than 20°C above the inversion. Veering winds are present below the inversion and backing winds above; both at speeds below 5 m s^{-1}.

Last, 24-h backward trajectories using a HYSPLIT 27-member ensemble (Stein et al. 2015) were calculated using NARR reanalysis data from the time and location of the Devil Fire to identify the source region of the dry air. The majority of ensemble members indicate an offshore origin with some back trajectories beginning as far north as the Oregon coastal waters, while some members offer a continental source region over northwestern California (Fig. 4b).

b. Climatology

A catalog of RAWS information and NDE count by site is presented in Table 1. A spatial representation of NDEs between 1 May and 31 October shows that the greatest propensity for nocturnal drying is across elevated coastal terrain of California south of Pt. Reyes (Fig. 5). The uneven distribution of NDEs along this geographic stretch is most evident in SFBA and makes the case that elevation is as important as geographic feature. SFBA and SC contain a diverse network of RAWS that allow for sampling at various altitudes and, in both of these regions, a general increase in NDEs is associated with an increase in elevation. The greatest number of summertime NDEs in the SFBA occur at the four uppermost RAWS in the region (MTD, RSP, MPC and BND) and are all at elevations above 710 m, or the mean height of the marine layer during summertime. Counts at these stations of 37, 22, 14, and 15 NDEs correspond to descending altitudes of 1173, 933, 792, and 712 m MS, respectively. The next closest site in this region is LSG with an average of four NDEs at elevation of 561 m MSL. Similar conditions exist in SC, where all RAWS above 900 m MSL averaged between 13 and 16 NDEs per summer and the highest site (MTW) had the most with 27 NDEs. At elevations below 900 m MSL, seasonal totals were five or less. Overall, NDEs are rarer in the NC and SN regions and are more likely related to dry frontal passages in SN.

Based on the greater frequency and summertime tendency of NDEs in the SFBA region, further analysis into seasonal and daily variability, as well as pertinent meteorological and fuel variables from MTD, RSP, MPC and BND was conducted. A very clear pattern emerges in both seasonal and diurnal occurrences of extremely dry air when looking at times when RH is below 9.5% and DP is less than or equal to −10.0°C. The overwhelming majority of extreme drying takes place between June and September at all four stations and the months of July and August account for approximately 40% of all occurrences (Fig. 6). A much less pronounced spike occurs during the winter months of December and January, most likely due to
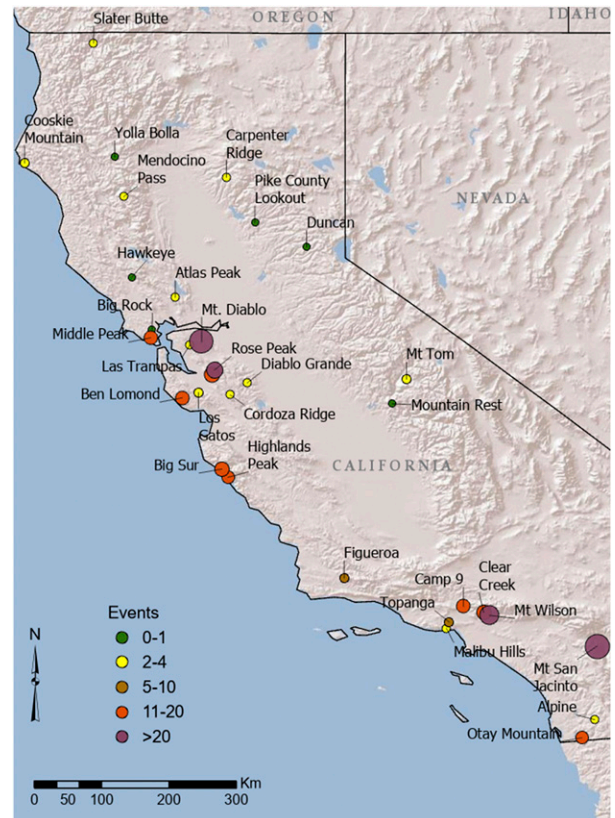
FIG. 5. Spatial extent and average number of NDEs between 1 May and 31 Oct 2000–14 for the region extending from Southern California to Oregon. Larger circles represent greater numbers of events (see legend).

cold frontal passages. The two locations closest to the coast show more of a seasonal delay, with a lower relative frequency of occurrence during June at MDC and BND than MTD and RSP, and vice versa during September. All four stations also exhibit a steep decline during October.

The diurnal pattern of NDEs is shown in Fig. 7 indicating the time at which such extremely dry air occurs at the same stations between 1 May and 31 October. A bimodal distribution of occurrences is evident that shows a maximum near midnight and minimum near 1400 PDT. At all locations, more than 75% of extreme drying takes place between 2000 and 0800 PDT and less than 10% between 1200 and 1600 PDT. The observed diurnal cycle in drying events is out of phase with the diurnal temperature cycle.

Wind roses from the four SFBA RAWS during NDEs are presented in Fig. 8 from times that satisfy the same criteria of simultaneous single-digit RH and DP below or equal to −10°C during 1 May–31 October. A consistent lack of an easterly wind component is apparent at each station and more representative of the typical west-northwesterly, onshore wind pattern around the SFBA. The two coastal locations, Middle Peak (MDP) (Fig. 8a) and Ben Lomond (BND) (Fig. 8c) have more of a northwesterly direction, which corresponds to the prevailing summertime winds along the coast (Neiburger 1960). Wind
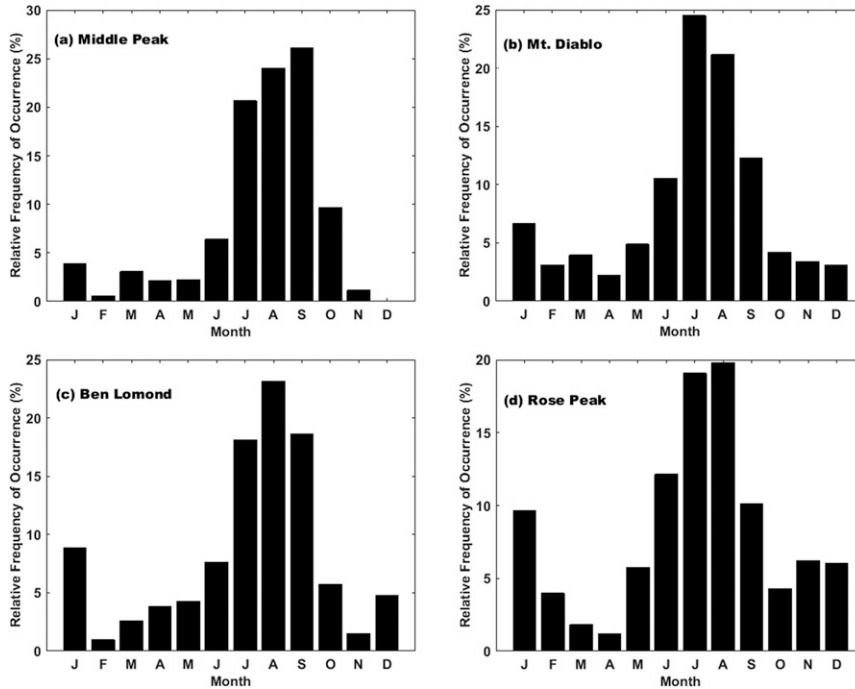
FIG. 6. Relative frequency of occurrence (%) by month when RH < 9.5% and DP ≤ −10°C for (a) Middle Peak, (b) Mount Diablo, (c) Ben Lomond, and (d) and Rose Peak between 2000 and 2014.

speeds of 5–10 m s^{-1} at MDP are greater than those at BND (<5 m s^{-1}) and Rose Peak (RSP) (Fig. 8d) has the greatest directional variability and lowest wind speeds of all four

stations. This could be partially due to the fact that it is the most sheltered site of the four, located in the upper slopes of an approximate north–south-oriented ridge and perpendicular
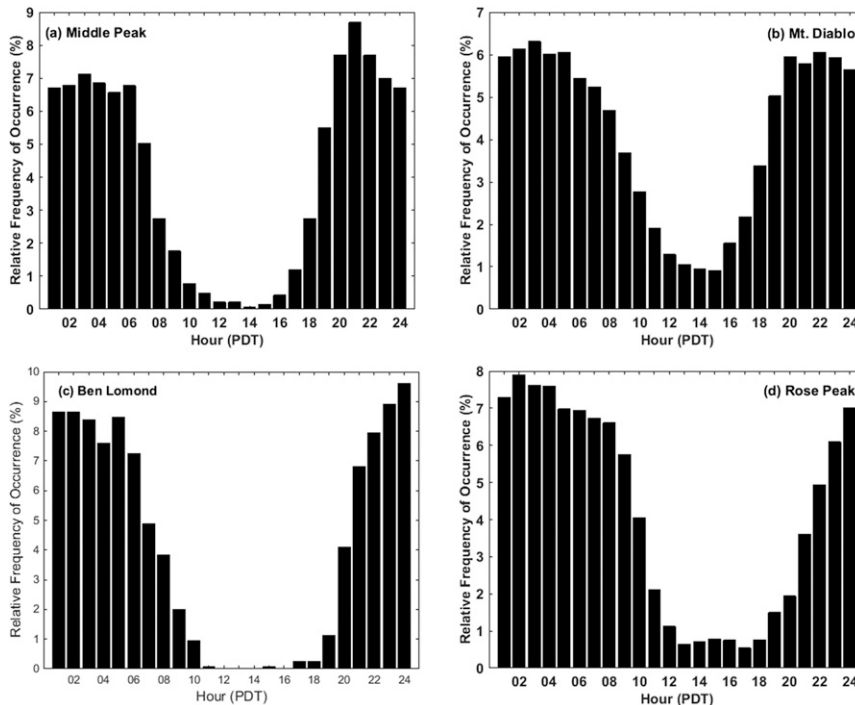
FIG. 7. As in Fig. 6, but for relative frequency of occurrence (%) by hour (PDT).
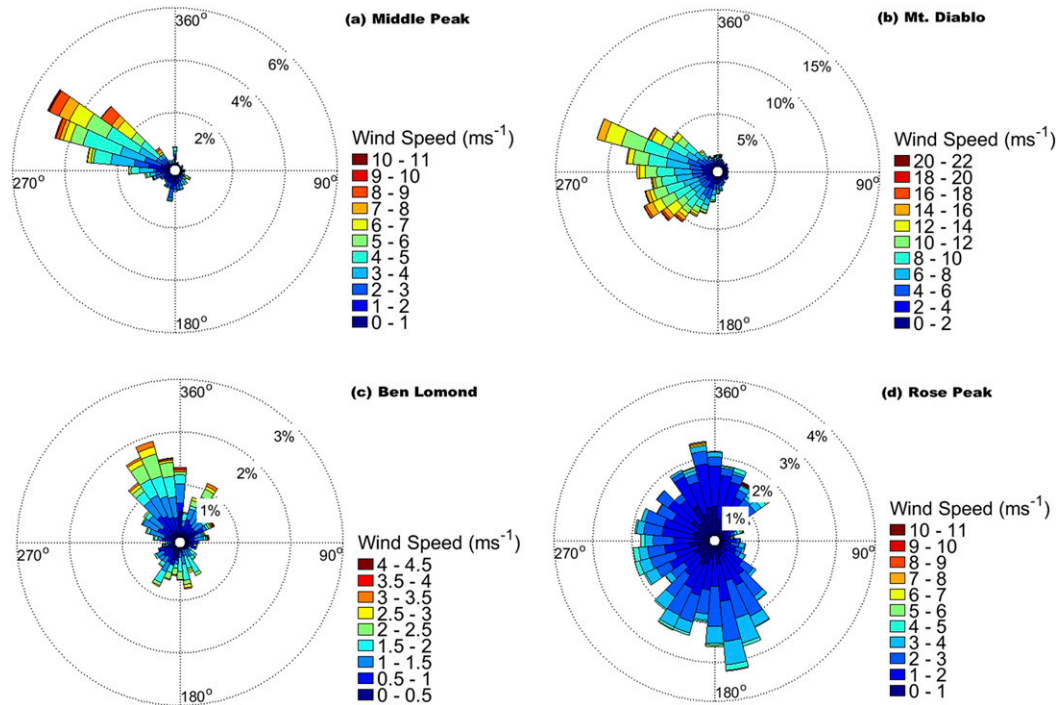
FIG. 8. Wind roses of wind speed (m s^{-1}) and direction for (a) Middle Peak, (b) Mount Diablo, (c) Ben Lomond, and (d) Rose Peak during NDEs from 1 May to 31 Oct 2000–14. Circles represent relative frequency of occurrence.

to a prevailing westerly flow. Conversely, the most exposed and elevated site of Mount Diablo (MTD) observes the strongest winds with prevailing directions between southeasterly and northwesterly (Fig. 8b).

Nocturnal drying events are outliers relative to most climatological statistics and have values well outside of 25th and 75th percentiles. Table 2 compares mean summer values of temperature, relative humidity, dewpoint temperature, wind speed, and 10-h fuel moisture to mean values of the same variables during NDEs from MTD, RSP, MDP and BND, and LTR. Mean summertime temperatures range between 18° and 20°C, but average closer to 21°–24°C during NDEs, which is still generally within upper percentile bounds. Greater discrepancies are found between normal summertime moisture characteristics and times of nocturnal drying. There is also an overall trend of decreasing RH with increasing station height. At the lowest elevation of 537 m, LTR has a mean summertime RH of 58%, while MTD averages just below 36% at an

elevation of 1173 m MSL. During NDEs, RH values average around 6% at all stations.

However, it is the lack of moisture, not temperature, responsible for driving such low RH during NDEs as seen in dewpoint temperatures in Table 2. Significant departures from summertime means on the order of 15°–20°C are present during NDEs. Normal values between 1° and 7°C drop closer to −20°C during NDEs and extreme values are below −35°C are common for all sites. Measurements of 10-h fuel moisture sensors from RAWS display characteristics similar to moisture variable and show a significant departure from normal during NDEs, with most values less than 5%.

Wind speeds offer less significant results and vary widely between stations. BND and RSP experience the lightest winds regardless of dry or normal conditions and generally remain below 5 m s^{-1}. This could partially be due to their more sheltered location, although the remaining three and more exposed sites only have average wind speeds closer to 5 m s^{-1}. MTD is

TABLE 2. Table of average summertime (1 May–31 Oct) and average NDE surface variables.

	Temperature		Relative humidity		Dewpoint		Wind speed		10-h fuel moisture	
	Summer	NDE	Summer	NDE	Summer	NDE	Summer	NDE	Summer	NDE
Las Trampas	18.3	23.6	57.7	6.3	7.4	−16.7	5.1	3.6	12.5	5.7
Ben Lomond	18.5	21.6	48.6	6.5	4.7	−17.7	1.9	1.4	8.9	4.1
Middle Peak	19.1	22.7	45.8	5.6	4.1	−18.9	4	3.7	9.4	4.1
Rose Peak	18.8	21.2	40.9	5.9	1.9	−19.6	2.5	1.8	10.3	8
Mount Diablo	18.8	22.3	36.1	5.5	−0.4	−19.9	6.9	8.3	7.5	3.3
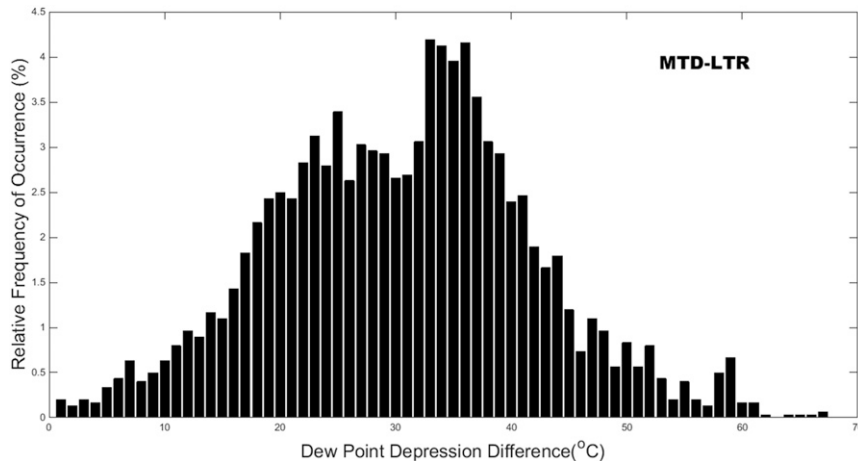
FIG. 9. Difference in dewpoint depressions between Mount Diablo and Las Trampas during NDEs and representing an elevation difference of 636 m.

the exception, with mean winds of 6 m s^{-1} and speeds close to 20 m s^{-1} during NDEs.

While the atmospheric conditions during NDEs can be similar regardless of location, the frequency of occurrence and magnitude of drying is much greater in higher elevations. Sharples et al. (2012) compared extreme drying events in Australia based on dewpoint difference anomalies between low-land and high-country locations. Similarly, our study looked at dewpoint depression differences between MTD and LTR during NDEs at MTD. These RAWS were chosen because they are very close in horizontal proximity but are located on separate ridges with an elevation difference of nearly 600 m between the two. The results shown in Fig. 9 show a drastic separation of extremely dry air and relatively moist air within that approximately 600 m elevation difference. During NDEs at MTD, dewpoint depression differences between the stations are between are typically between 20° and 40°C and can reach close to differences of 65°C (Fig. 9). In fact, the frequency of occurrences with dewpoint depression differences greater than 50°C is the same as those below 10°C.

c. Synoptic composite

There have been cases of significant overnight drying occurring in multiple locations throughout the SFBA at the same time, as well as reaching abnormally low levels. To further understand the environment under which more significant NDEs occur, large-scale momentum, temperature, and moisture characteristics of the atmosphere were investigated before, during, and after the most critical periods of nocturnal drying in the SFBA. Over the course of 11 summers between 2004 and 2014, 87 significant NDEs were identified.

The evolution of such episodes is revealed by comparing specific features in the synoptic composites using NAM-218 data. The first composite analysis of interest is that of MSLP overlaid with 500-hPa heights (Fig. 10) and shows the synoptic progression surrounding significant nocturnal drying events in the SFBA. First, a shortwave trough of low pressure can be seen in the 500-hPa height field amplifying as it approaches

Northern California in the 36 h prior to event onset, while an upper-level ridge of high pressure simultaneously builds across the interior western United States (Fig. 10a). The base of this trough is situated around 37°N and 145°W with an adjacent area of high pressure centered over northern Mexico. By $T = 0$, the trough axis extends and shifts southeastward to 35°N and 137°W (Fig. 10c) as high pressure is displaced slightly eastward. By $T + 12$, meridional flow at the 500-hPa level is at its greatest with a well-defined trough along the West Coast and a ridge of high pressure extending from the Four Corners region into southwestern Canada (Fig. 10d).

The opposite scenario is presented at the surface where an area of high pressure centered near 37°N and 145°W dominates the northeastern Pacific and a thermal low resides over the Desert Southwest (Fig. 10). At $T − 36$ before the event, the northeastern periphery of a high pressure system extends into British Columbia, Washington, and Oregon representing a West Coast thermal trough associated with intense daytime heating as described by Brewer (Brewer et al. 2012). As the upper-level trough of low pressure moves eastward, high pressure at the surface gradually weakens and shifts southward (Figs. 10a–d). The surface-based high pressure ridge extending into the Pacific Northwest, although still evident the day following the event (Fig. 10d), is less prominent and positioned farther south and west than at $T − 36$. The surface area of low pressure over the southwestern United States can be attributed to strong diabatic heating and is a common summertime feature of the region (Whiteman 2000). Little change is observed during event progression of the thermal low, except a slight eastward displacement. The juxtaposition of the northeast Pacific high and Desert Southwest low creates a strong pressure gradient off the West Coast. The region of tightest pressure gradients also moves south from the Northern California and southern Oregon coastal border to waters off the central California coast.

This synoptic environment allows for strong subsidence along the California coast, drawing extremely dry air from upper to lower levels of the troposphere. The first ingredient
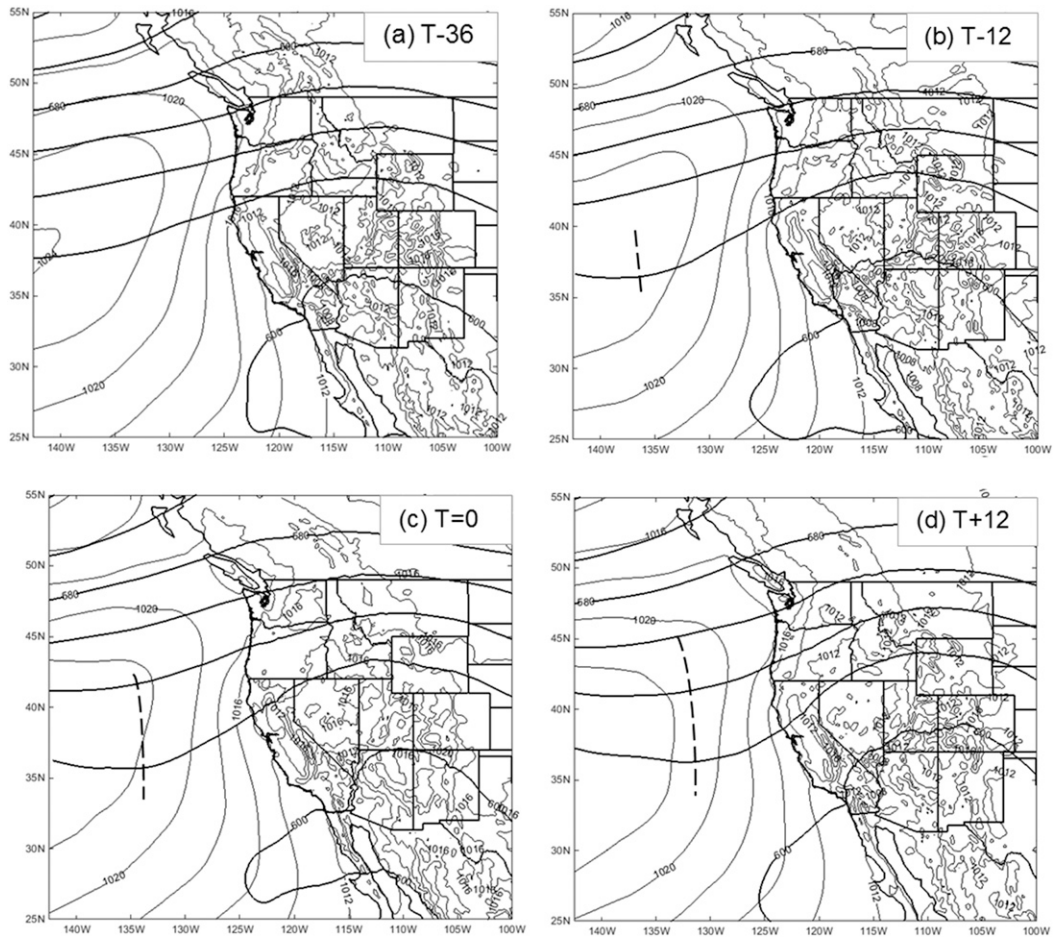
FIG. 10. Composites of 500-hPa heights (thick) and MSLP (thin) of 83 significant NDEs from the SFBA at (a) 36 h prior to, (b) 12 h prior to, (c) during, and (d) 12 h after each event. The trough axis is indicated by the dashed line.

for downward vertical motion and subsequent dry air is low-level divergence around the eastern periphery of the Pacific high. The 925-hPa level divergence (Fig. 11a) shows an area of

maximum divergence over western Oregon spreading off the Northern California coast to the south in a wedge-like shape between 120° and 130°W. The strong divergence in this region
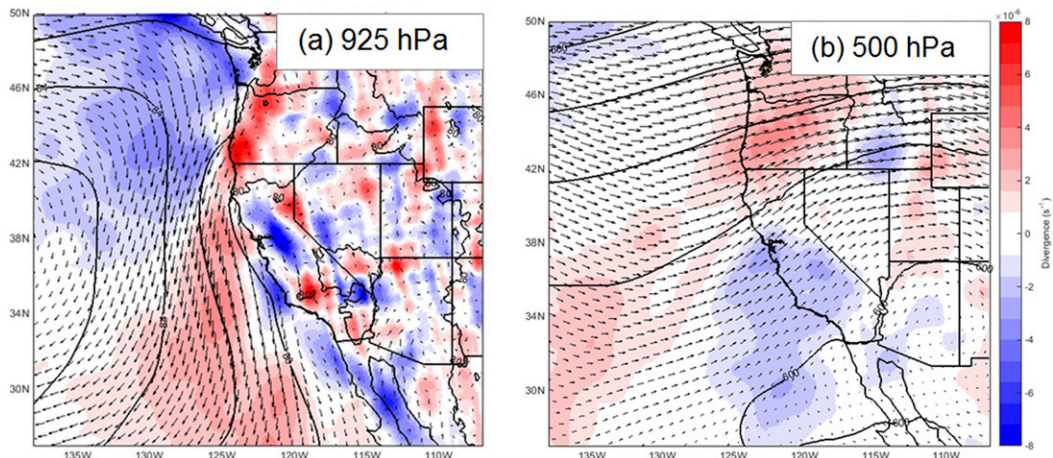
FIG. 11. Composites of 925- and 500-hPa heights (contours), convergence, and divergence (shading) of 83 significant NDEs from the SFBA at $T = 0$.
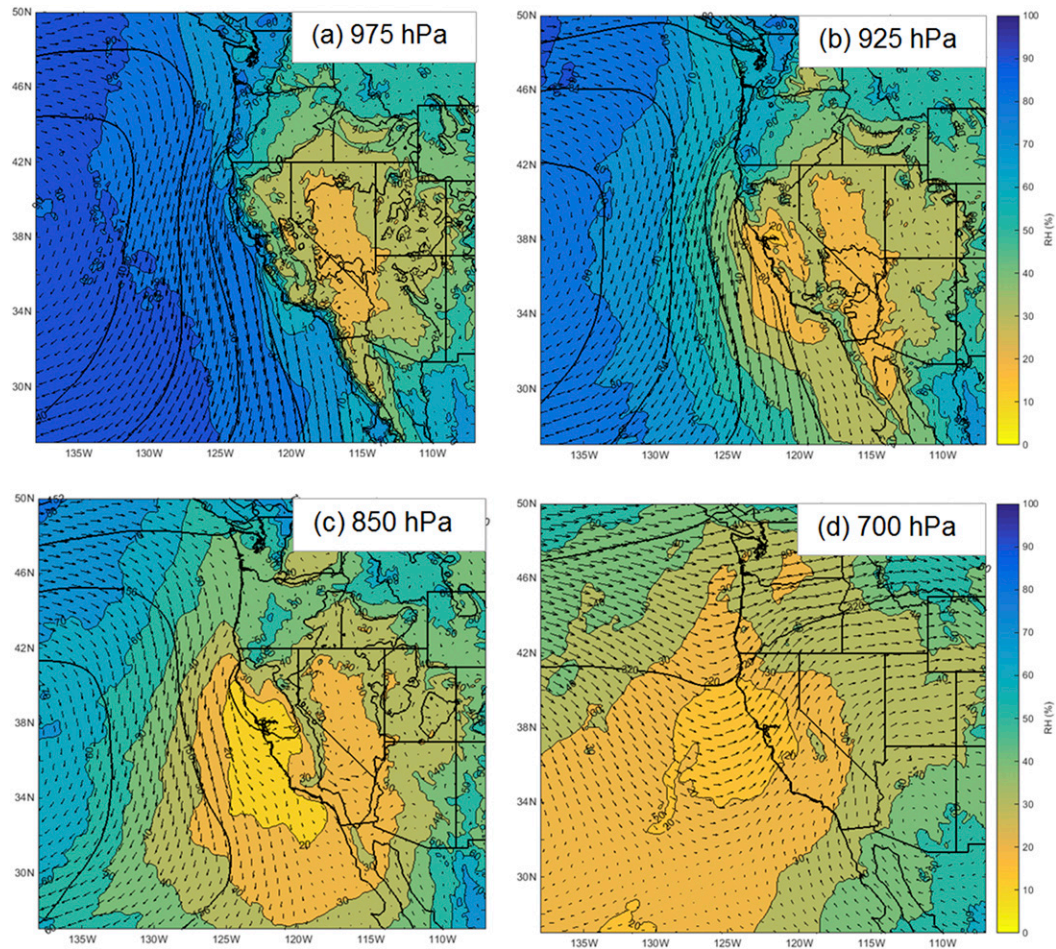
FIG. 12. Composites of 975-, 925-, 850-, and 700-hPa heights (contours), winds (vectors), and RH (shading) of 83 significant NDEs from the SFBA at $T = 0$.

is associated with a LLJ caused from pressure differences between high pressure to the west and low pressure to the east. Winds up to $11\,\mathrm{m\,s^{-1}}$ are found in the low-level jet and corresponding areas of divergence that both get displaced southward as the anticyclone weakens during event evolution. Areas of convergence around California can be attributed to the blocking effects of coastal terrain and surface friction (Burk and Thompson 1996).

In the upper levels, an approaching upper-level trough provides another possible component for enhanced low-level subsidence with an area of convergence present over the SFBA. Figure 11b shows areas of divergence in the Pacific Northwest and convergence over California during NDEs associated with a trough over the northeastern Pacific and a ridge of high pressure over the Intermountain West.

RH at various pressure levels shows evidence of very dry air associated with the subsidence-inducing factors of low-level divergence and upper-level convergence (Fig. 12). In the lower troposphere, the driest air is isolated to an area just off the central and Southern California coast above the marine layer, as indicated by RH values above 70% in the 975-hPa level.

While low RH across the interior can be attributed to warmer temperatures, the region of dry air along California corresponds to the area of divergence at the 925- and 850-hPa pressure levels and can be associated with subsidence. A much larger region of dry air is present off the California coast at 850 hPa that almost reaches the length of the entire state (Fig. 12c) and it is at this level where the driest air is found. Similar to 925-hPa RH, an inland intrusion occurs through the SFBA and it should be no coincidence that the deepest inland extent of dry air occurs over the greater SFBA due to experimental design. A pocket of low RH over the California coast is even evident up to 700 hPa (Fig. 12d). During periods associated with significant NDEs, the driest air west of the Rocky Mountains at the 850-hPa level can be found off the California coast.

d. Upper-air sounding

A pressure-averaged composite of 12Z KOAK soundings during 87 significant NDEs in the SFBA reveals an exaggerated Y-shaped temperature and dewpoint profile as a layer of extremely warm and dry air with dewpoint depressions greater
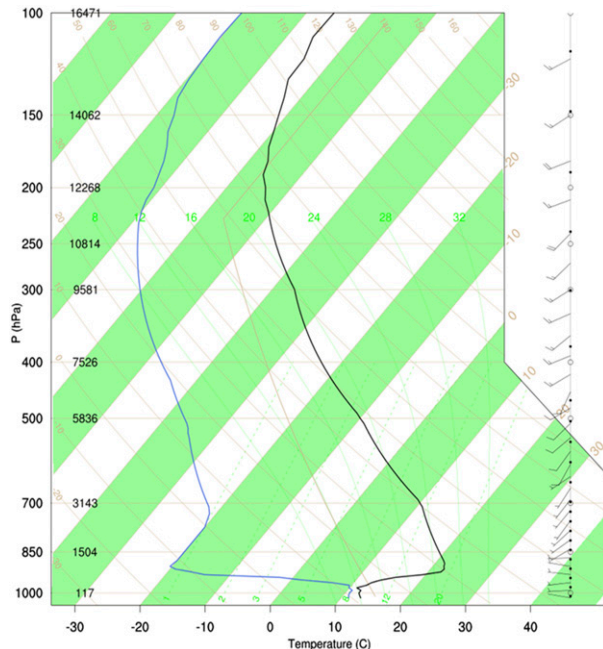
FIG. 13. Composite sounding from KOAK of temperature (black), dewpoint (blue), and wind barbs (m s^{-1}) during 69 significant SFBA NDEs.

FIG. 14. Composite sounding from KOAK of potential temperature (red) and mixing ratio (blue) during significant SFBA NDEs.

than 40°C exists immediately above a shallow marine layer with associated dewpoint depressions less than 3°C (Fig. 13). Temperatures around 13°C at the surface reach 22°C at the inversion top (925 hPa), while conversely, dewpoint temperatures drop from 10° to −20°C through the inversion. Lapse rates in the inversion on the order of 20°C km^{-1} for temperatures and −60°C km^{-1} for dewpoint temperatures. An overall onshore wind pattern is exhibited through the entire sounding. Westerly winds below 5 m s^{-1} near the surface turn to a south-southwesterly direction above the inversion top, and then transition to a more west-southwesterly direction above 500 hPa where speeds increase to between 10 and 20 m s^{-1}.

The inversion base begins above the marine layer at 364 m MSL and continues to a height of 824 m MSL as indicated by the stable layer in the potential temperature profile shown in Fig. 14. The mixing ratio profile intersects the potential temperature profile near the middle of the inversion as values drop from 8 g kg^{-1} in the marine layer to 1.3 g kg^{-1} above the inversion.

4. Discussion and summary

An abrupt and dramatic overnight decrease in RH resulted in the unexpected and explosive growth of the Devil wildfire on 29 August 2003 that overran crews and forced the largest fire shelter deployment in California history. The location was near the San Francisco Bay Area in a remote area of the Diablo Range, a rugged mountain chain that extends down the coastal interior of central California. Higher coastal elevations across central California are plagued by episodes of severe and often sudden onset of nocturnal drying. Relative humidity values

below 0.5%, dewpoint temperatures of −40°C, and mixing ratios less than 0.5 g kg^{-1} have been measured in these elevated locations. Nocturnal drying events are a major concern for fire management agencies because they can result in extreme fire behavior and pose a great threat to firefighters, but they are still poorly understood.

A basic set of qualifications based on the meteorological conditions during the Devil Fire entrapment was used to identify and investigate such events (RH < 9.5% and dewpoint temperatures ≤ −10°C for at least 3 h between 2000 and 0800 PDT). A climatology identified the spatial and temporal extent of NDEs in California. Synoptic composites of pressure levels and upper-air soundings revealed the larger-scale mechanisms leading to the formation of dry air and event evolution. A detailed case study was performed of the Devil Fire shelter deployment. Key findings from this study include the following:

- A source region of extremely dry air at the 850-hPa level associated with large-scale subsidence over the northeastern Pacific exists. Subsidence is enhanced by an elongated LLJ in an area within a few hundred kilometers of the California coast.
- The dry air exists in a layer located directly above the marine inversion, and they both advect inland overnight. An upper-level trough of low pressure amplifying along the West Coast of the United States promotes onshore advection and is associated with periods of significant nocturnal drying in upper elevations.
- NDEs are more pronounced in the SFBA where terrain gaps are present in the coastal barrier, especially in higher elevations, but are also common in California coastal terrain south of 40°N.
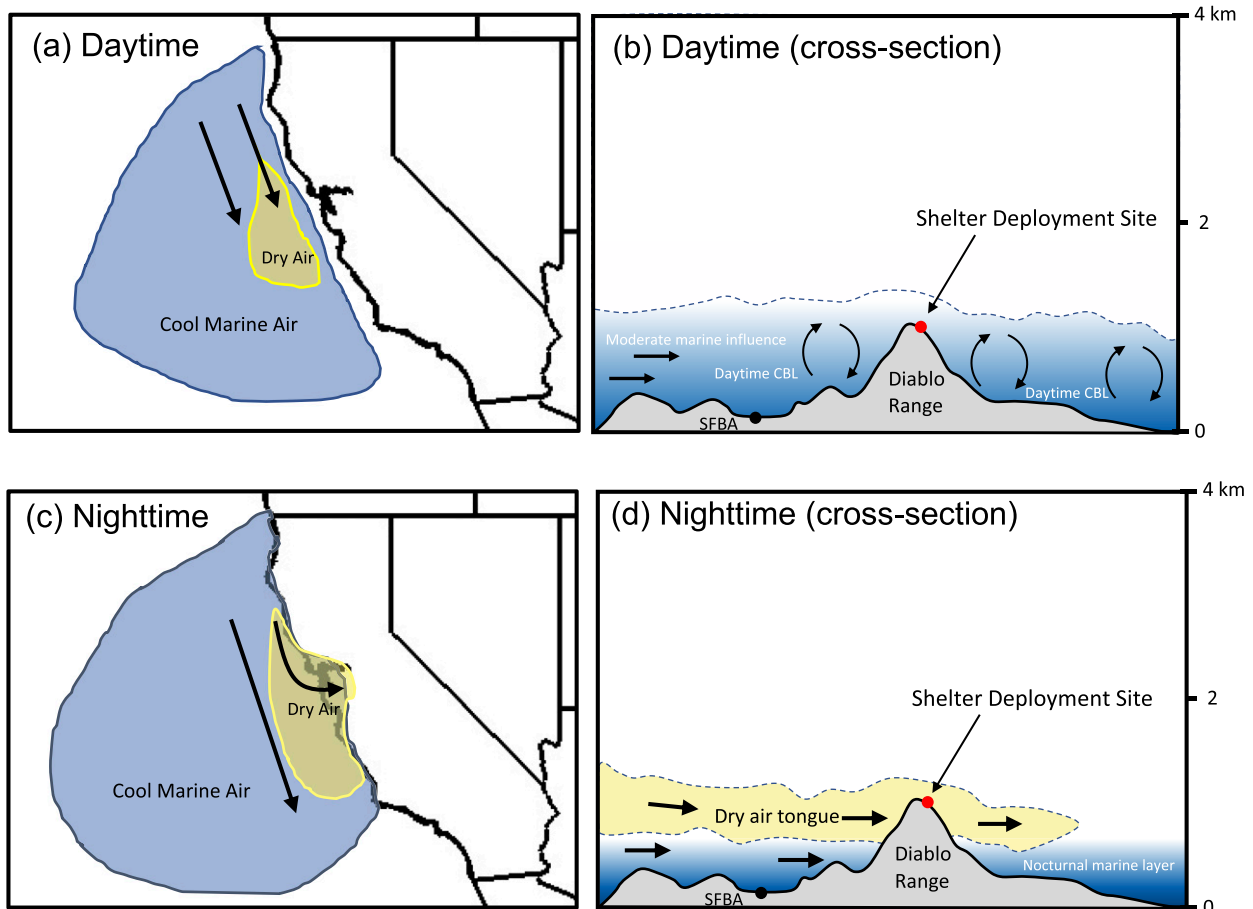
FIG. 15. Conceptual model of NDEs and their diurnal evolution. Blue shading represents cool, moist marine air, and yellow shading represents warm and dry air aloft. Arrows are generalized wind vectors. The SFBA and shelter deployment site are shown.

A synoptic composite of 87 significant NDEs from the SFBA revealed key features in large-scale dynamics responsible for the formation of dry air and how NDEs evolve. Surface high pressure over the northeastern Pacific and a thermal low pressure area in the southwestern United States create a baroclinic marine inversion along the California coast. Above this inversion, a low-level jet develops, creating substantial divergence at the 925-hPa level, subsidence in the lower troposphere, and strengthening of the marine inversion. An 850-hPa source region of dry air accompanied this region of low-level divergence, an extension of which advects through coastal barriers overnight with the marine layer. More significant NDEs are associated with an inland push of stratus as a weak upper-level shortwave trough of low pressure moves across the Pacific Northwest, causing the eastern Pacific subtropical high and thermal trough along the West Coast to weaken. Furthermore, upper-level convergence aloft associated with the approaching low pressure trough enhanced subsidence over the SFBA while ushering in a separate source of dry air in the middle troposphere from latitudes south of 35°.

Based on the analysis of the identified NDEs and the case study of the Devil Fire, an idealized conceptual model representing the processes of how dry air above the marine layer intrudes inland and collapses upon higher terrain at night are responsible for NDEs is presented in Fig. 15. During daytime, the dry air aloft is located offshore and above the marine layer (Fig. 15a). Over land, the convective boundary layer develops and is associated with moderate to weak marine layer influence. This boundary layer air brings moisture from lower altitudes to the higher elevations of the Coastal Ranges as depicted in Fig. 15b. At night, a strong marine layer advects into the interior valleys of the SFBA (Fig. 15c). Above this shallow nocturnal marine layer, the extremely dry air that was present offshore earlier is coupled to the marine layer and also advects into the region and impinges on the higher-elevation terrain of the SFBA causing extreme drying during overnight hours (Fig. 15d). This often occurs when there are shallow stratocumulus clouds present at the top of the marine layer.

There are many characteristics to nocturnal drying. The events described in this study portray some of the more drastic conditions, but nighttime drying events exhibit much variation. Overall, NDEs are more pronounced in coastal terrain above 800 m MSL south of Point Arena, but are possible as low as 450 m MSL. Event duration can last from an hour at a minimum or persist all night and some cases can continue for several consecutive nights. However, high-resolution forecast

models struggle to capture the extent of drying above the inversion, making it difficult to forecast NDEs in an operational setting or in terms of fire danger.

This study showed that transition from very low fire danger to extreme fire danger can occur overnight and that NDEs are a common summertime feature in the elevated terrain of coastal California. Future work will include high-resolution numerical simulations based on this study to better understand the dynamics and evolution of NDEs. It is our hope that improved understanding of NDEs will likely lead to increased firefighter and community safety in regions where NDEs occur.

REFERENCES

Brewer, M. C., C. F. Mass, and B. E. Potter, 2012: The West Coast thermal trough: Climatology and synoptic evolution. *Mon. Wea. Rev.*, **140**, 3820–3843, https://doi.org/10.1175/MWR-D-12-00078.1.

Brotak, E. A., and W. E. Reifsnyder, 1977: An investigation of the synoptic situations associated with major wildland fires. *J. Appl. Meteor.*, **16**, 867–870, https://doi.org/10.1175/1520-0450(1977)016<0867:AIOTSS>2.0.CO;2.

Burk, S. D., and W. T. Thompson, 1996: The summertime low-level jet and marine boundary layer structure along the California coast. *Mon. Wea. Rev.*, **124**, 668–686, https://doi.org/10.1175/1520-0493(1996)124<0668:TSLLJA>2.0.CO;2.

California Department of Forestry and Fire Protection, 2003: Wildland fire entrapment fire shelter deployment review. California Department of Forestry and Fire Protection Review Rep., 8 pp.

Cohen, J. D., and J. E. Deeming, 1985: The National Fire-Danger Rating System: Basic Equations. U.S. Department of Agriculture Forest Service Pacific Southwest Forest and Range Experiment Station Tech. Rep. PSW-82, 23 pp., https://www.fs.fed.us/psw/publications/documents/psw_gtr082/psw_gtr082.pdf.

Fosberg, M., 1978: Weather in wildland fire management: The fire weather index. *Proc. Conf. on Sierra Nevada Meteorology*, Lake Tahoe, CA, Amer. Meteor. Soc. and USDA Forest Service, 1–4.

Haines, D. A., 1989: A lower atmosphere severity index for wildlife fires. *Natl. Wea. Dig.*, **13**, 23–27.

Horel, J., and Coauthors, 2002: Mesowest: Cooperative Mesonets in the Western United States. *Bull. Amer. Meteor. Soc.*, **83**, 211–226, https://doi.org/10.1175/1520-0477(2002)083<0211:MCMITW>2.3.CO;2.

Huang, C., Y.-L. Lin, M. L. Kaplan, and J. J. Charney, 2009: Synoptic-scale and mesoscale environments conducive to

forest fires during the October 2003 extreme fire event in Southern California. *J. Appl. Meteor. Climatol.*, **48**, 553–579, https://doi.org/10.1175/2008JAMC1818.1.

Hughes, M., and A. Hall, 2010: Local and synoptic mechanisms causing Southern California's Santa Ana winds. *Climate Dyn.*, **34**, 847–857, https://doi.org/10.1007/s00382-009-0650-4.

Mills, G. A., 2008a: Abrupt surface drying and fire weather Part 1: Overview and case study of the South Australian fires of 11 January 2005. *Aust. Meteor. Mag.*, **57**, 299–309.

——, 2008b: Abrupt surface drying and fire weather Part 2: A preliminary synoptic climatology in the forested areas of southern Australia. *Aust. Meteor. Mag.*, **57**, 311–328.

Munns, E. N., 1921: Evaporation and forest fires. *Mon. Wea. Rev.*, **49**, 149–152, https://doi.org/10.1175/1520-0493(1921)49<149:EAFF>2.0.CO;2.

Neiburger, M., 1960: The relation of air mass structure to the field of motion over the Eastern North Pacific Ocean in Summer 1. *Tellus*, **12**, 31–40, https://doi.org/10.1111/j.2153-3490.1960.tb01281.x.

Pilié, R., E. Mack, C. Rogers, U. Katz, and W. Kocmond, 1979: The formation of marine fog and the development of fog-stratus systems along the California coast. *J. Appl. Meteor.*, **18**, 1275–1286, https://doi.org/10.1175/1520-0450(1979)018<1275:TFOMFA>2.0.CO;2.

Potter, B. E., 2012: Atmospheric interactions with wildland fire behaviour—I. Basic surface interactions, vertical profiles and synoptic structures. *Int. J. Wildland Fire*, **21**, 779–801, https://doi.org/10.1071/WF11128.

Raphael, M., 2003: The Santa Ana winds of California. *Earth Interact.*, **7**, https://doi.org/10.1175/1087-3562(2003)007<0001:TSAWOC>2.0.CO;2.

Schroeder, M. J., and Coauthors, 1964: Synoptic weather types associated with critical fire weather. U.S. Department of Agriculture Forest Service Pacific Southwest Forest and Range Experiment Station Rep., 503 pp., https://www.fs.usda.gov/treesearch/pubs/44220.

Sharples, J., G. Mills, and R. McRae, 2012: Extreme drying events in the Australian high-country and their implications for bushfire risk management. *Aust. Meteor. Oceanogr. J.*, **62**, 157–170, https://doi.org/10.22499/2.6203.004.

Srock, A. F., J. J. Charney, B. E. Potter, and S. L. Goodrick, 2018: The hot-dry-windy index: A new fire weather index. *Atmosphere*, **9**, 279, https://doi.org/10.3390/atmos9070279.

Stein, A., R. R. Draxler, G. D. Rolph, B. J. Stunder, M. Cohen, and F. Ngan, 2015: NOAA's HYSPLIT atmospheric transport and dispersion modeling system. *Bull. Amer. Meteor. Soc.*, **96**, 2059–2077, https://doi.org/10.1175/BAMS-D-14-00110.1.

Walbrun, R., and W. Blier, 2004: An examination of a lightning event in the San Francisco Bay Region using the weather event simulator. National Weather Service WFO Monterey Doc., 8 pp., https://www.weather.gov/media/wrh/online_publications/talite/talite0425.pdf.

Werth, P. A., and Coauthors, 2011: Synthesis of knowledge of extreme fire behavior: Volume I for fire managers. U.S. Department of Agriculture Forest Service Pacific Northwest Research Station Tech. Rep. PNW-GTR-854m, 144 pp., https://doi.org/10.2737/PNW-GTR-854.

Whiteman, C. D., 2000: *Mountain Meteorology: Fundamentals and Applications.* Oxford University Press, 376 pp.